

## Determination of Aluminium-26 in Biological Materials by Accelerator Mass Spectrometry

S. J. King<sup>a</sup>, C. Oldham<sup>a</sup>, J. F. Popplewell<sup>a</sup>, R. S. Carling<sup>a</sup>, J. P. Day<sup>\*a</sup>, L. K. Fifield<sup>b</sup>, R. G. Cresswell<sup>b</sup>, Kexin Liu<sup>b</sup> and M. L. di Tada<sup>b</sup>

<sup>a</sup> Department of Chemistry, University of Manchester, Manchester, UK M13 9PL

<sup>b</sup> Department of Nuclear Physics, Australian National University, Canberra, ACT 0200, Australia

E-mail: philip.day@man.ac.uk

**Studies of the biological chemistry of aluminium can gain significantly from the use of the long-lived isotope <sup>26</sup>Al as a tracer, although the cost of the isotope often precludes its determination by radiochemical counting techniques. Accelerator mass spectrometry (AMS) provides an ultra-sensitive method of determination, free from isobaric interference from atomic (<sup>26</sup>Mg) or molecular species. The source materials for AMS can be aluminium oxide or phosphate, both of which can be readily prepared at a sufficient level of purity from biological substrates. Natural aluminium (<sup>27</sup>Al, 100%) is added to the preparations as a chemical yield monitor and to provide the reference for the isotope ratio measurement. <sup>26</sup>Al/<sup>27</sup>Al ratios can be determined over the range 10<sup>-14</sup>–10<sup>-7</sup>, implying a limit of detection for <sup>26</sup>Al of around 10<sup>-18</sup> g. The precision of measurement and long-term reproducibility are <5% and <7% (RSD), respectively. Chemical methodologies for routine measurements on blood and urine samples have been developed.**

**Keywords:** Accelerator mass spectrometry; aluminium-26; biological analysis

Over the past 20 years, aluminium has emerged as an important toxic element, both in human medicine and in the wider environment as a consequence of acidic precipitation.<sup>1</sup> However, until recently, the study of the biological chemistry of aluminium was hampered by the lack of a suitable tracer isotope. Natural aluminium is monoisotopic (<sup>27</sup>Al; Table 1) and, of the accessible radioisotopes, only <sup>26</sup>Al is sufficiently long-lived for its practical use in tracer experiments in living systems. However, the combination of high cost and low specific activity render this isotope too expensive for general use as a radiotracer, and the potential isobaric interference from the abundant magnesium isotope, <sup>26</sup>Mg, makes the use of conventional mass spectrometry (even at high resolution) all but impracticable.

The isobar problems can, in principle, be overcome by the use of accelerator mass spectrometry,<sup>2</sup> and since the late 1980s developments in this technique have facilitated a number of biological and biomedical studies, many involving human subjects.<sup>3</sup> The chemical methodology needed to couple biological experiments to the sophisticated physics of AMS

measurement has certain unique characteristics, and it is the object of this paper to explain, justify and quantify the procedures which have been developed.

AMS is a mass spectrometric technique for the determination of trace amounts of stable or long-lived radioactive isotopes, in which a tandem electrostatic particle accelerator is coupled to a number of magnetic, and sometimes also electrostatic, dispersing elements.<sup>2</sup> The concentration of the rare isotope of interest is measured by identifying and counting individual monatomic ions with nuclear detection techniques after acceleration to energies in the MeV range. By comparing the counting rate with the ion current of one of the element's major isotopes, the concentration of the rare isotope can be determined. The principal attributes of the technique are an extremely high sensitivity, almost total selectivity and an exceptionally wide range of isotope concentration measurement. Detection limits down to a few thousand atoms are achievable, often against measurement backgrounds near to zero and, in contradistinction to conventional mass spectrometry, isobaric and molecular interferences can be completely eliminated. Isotope ratio measurements in the range 10<sup>-14</sup>–10<sup>-7</sup> are readily achievable.

Historically, the major applications of AMS have been to the natural environment, associated with the measurement of long lived cosmogenic radionuclides.<sup>4,5</sup> The most widely applied isotope is <sup>14</sup>C, with applications ranging from archaeological dating to studies of global climate change, and in these applications the use of AMS has greatly extended the sensitivity of <sup>14</sup>C determination over more traditional radiochemical methods.<sup>6</sup> Extensive use has also been made of the isotopes <sup>10</sup>Be, <sup>26</sup>Al and <sup>36</sup>Cl for studies of landscape evolution and hydrology.<sup>5</sup> More recently, the technique has been applied to biological research, using artificially produced long lived radionuclides in isotopic tracer studies. In this area, the ultrasensitivity of AMS has proved a particularly valuable asset, allowing the use of such tracers in human studies at acceptably low radiation doses. Successful applications using <sup>14</sup>C,<sup>7</sup> <sup>41</sup>Ca,<sup>8</sup> and <sup>26</sup>Al<sup>3,9–13</sup> have been reported, and we have recently extended the potential biomedical use of AMS to the actinide nuclides.<sup>14,15</sup>

The first application of <sup>26</sup>Al AMS to tracer studies in humans was carried out at the University of Manchester, using the accelerator at the late UK Nuclear Structure Facility, Daresbury.<sup>9</sup> Following the closure of this accelerator in 1993, this research programme has been continued in a collaboration between the Manchester group and the Department of Nuclear Physics, Australian National University (ANU).<sup>16</sup> The methodology of the AMS technique now described is that currently employed for <sup>26</sup>Al measurements at the ANU.

**Table 1** The isotopes of aluminium

Isotope mass number	Radioactive half-life
25	7.2 s
26	716 000 y
27	Stable
28	2.3 min
29	6.6 min

### Accelerator Mass Spectrometry

#### Principles

In the most common AMS configuration, negative ions of the tracer isotope and its abundant stable counterpart(s) are

generated in a Cs sputter source, passed through a magnetic sector and accelerated through a potential of several MV to a positive terminal. At the terminal, passage through a thin foil or low pressure gas generates positive ions of high charge, which then accelerate back to ground potential, where they pass through further electrostatic and magnetic selection. Individual ions of the tracer isotope are counted by standard high-energy nuclear detection techniques, and the abundant isotope is quantified by measurement of its beam current at some point in the system.

The AMS system, as applied to  $^{26}\text{Al}$  at the Australian National University, is shown schematically in Fig. 1.<sup>17</sup> In outline, its mode of operation is as follows.

1. An ion source produces negative ions from a suitable aluminium-containing compound, generally aluminium oxide ( $\text{Al}_2\text{O}_3$ ). The negative ion beam contains, amongst others, the ion species of interest,  $\text{Al}^-$ .

2. A first magnetic analysis (the injector magnet) selects ions of the required mass-to-charge ratio, in this case  $m/z$  26 or 27 (the magnetic field is cycled between the two settings and the isotopes are selected alternately).

3. These ions are accelerated to the positive high voltage terminal of the accelerator, where they pass through a very thin (approximately  $5 \mu\text{g cm}^{-2}$ ) carbon foil. Atomic species, such as  $\text{Al}^-$ , are stripped of several electrons, and the resulting positive ions experience a further acceleration back to ground potential. At the ANU, an accelerating potential of 11.4 MV is used for  $^{26}\text{Al}$  analysis, and under these conditions about 30% of the  $^{26}\text{Al}$  ions are in the 7+ charge state after stripping, with the majority of the remainder distributed over the range +5 to +9. Most importantly, any molecular ions which passed the first magnetic analysis are fully dissociated and partially stripped of electrons, giving a range of positive ions, mostly of low mass, which are also further accelerated.

4. After acceleration, a further high resolution magnetic analysis (the analysing magnet) selects the ionic species of interest at a well defined energy. In our example, this would be

either  $^{26}\text{Al}^{7+}$  or  $^{27}\text{Al}^{7+}$  at about 90 MeV. Ions originating from molecular fragments do not in general have the correct magnetic rigidity to pass this analysis, although charge exchange processes during transit may result in a small proportion of anomalous ions passing the analysing magnet. Included in this are small amounts of  $^{25}\text{Mg}$  (from  $^{25}\text{MgH}^-$ ) and  $^{26}\text{Mg}$  (from  $^{26}\text{MgH}^-$ ), which accompany  $^{26}\text{Al}$  and  $^{27}\text{Al}$ , respectively.

5. Finally, the accelerated ions are detected in a gas ionisation chamber, which is able to identify each arriving ion unambiguously. It does this by measuring the total energy of the ion, and by making multiple measurements of the energy loss (which is in part dependent on nuclear charge) as the ion slows in the detector gas. Each species thus occupies a unique position in a multi-dimensional space, in marked contrast to low-energy mass spectrometry, where a detector capable of detecting individual ions is not able to discriminate between, say,  $^{26}\text{Al}$  and  $^{26}\text{Mg}$ , or more generally,  $^{26}\text{Al}$  and molecular ions of  $m/z$  26.

6. Since the quantity of interest is the isotope ratio,  $^{26}\text{Al}/^{27}\text{Al}$ , it is also necessary to measure the intensity of the stable isotope. In our system, this is done periodically by switching the first (low-energy) mass analysis to mass 27 and changing the terminal voltage to 11.0 MV, in order to give  $^{27}\text{Al}^{7+}$  ions the same magnetic rigidity as the  $^{26}\text{Al}^{7+}$  ions (the corresponding energy is 88 MeV). In this way, the  $^{27}\text{Al}^{7+}$  ions can be transmitted to a Faraday cup inserted (during the  $^{27}\text{Al}$  cycle) immediately in front of the ionisation detector. The  $^{27}\text{Al}^{7+}$  intensity is thus measured as an ion current.

7. There are also a number of electrostatic and magnetic quadrupole lenses and steerers, used to optimise transmission of the Al beam through the machine from the ion source to the detector, and a recently added velocity filter (Wien filter) after the analysing magnet, which is set to select against extraneous ions accompanying  $^{26}\text{Al}$  or  $^{27}\text{Al}$ . The overall transmission efficiency of the machine is 14%, which is largely determined by the abundance (about 30%) of the 7+ charge state.

## Ion Source

### Ion production

So far, a first generation caesium sputter source (Hiconex Model 832<sup>18</sup>) has been used for biological AMS. Samples of  $\text{Al}_2\text{O}_3$  (typically 0.2–5 mg) are mixed with approximately the same mass of silver powder (which serves as an electrical and thermal conductor) and packed into 2 mm stainless-steel grub screws inserted into cylindrical copper blocks (approximately 1 cm  $\times$  1 cm diameter). These blocks are loaded into a 12-position sample wheel and mounted in the ion source. Negative ions are produced as a result of bombarding the  $\text{Al}_2\text{O}_3$ –Ag surface under high vacuum with a beam of 22 keV  $\text{Cs}^+$  ions. The beam both dislodges atomic/molecular ions from the surface and deposits Cs atoms. The deposited Cs (which has a very low ionisation energy) facilitates electron transfer from the cathode to emerging ions, promoting the formation (in order of abundance) of  $\text{O}^-$ ,  $\text{Ag}^-$ ,  $\text{AlO}^-$ ,  $\text{Al}^-$  and other negative ions, which are extracted by the applied electric field. Typically, beam currents of up to 50 and 500 nA for the ions  $\text{Al}^-$  and  $\text{AlO}^-$ , respectively, are produced from the  $\text{Al}_2\text{O}_3$ –Ag mixture. The negative ion beam may also include  $\text{MgO}^-$ ,  $\text{MgH}^-$ ,  $\text{BO}^-$ ,  $\text{C}_2^-$ ,  $\text{CN}^-$  and other ions from impurities in the source material. However, although Mg, which is a common biological element, may well be present in macroscopic amounts (up to 1%) in the  $\text{Al}_2\text{O}_3$ , the ion  $\text{Mg}^-$  is not stable and is, therefore, not present to any extent in the beam, an exclusion which is of major importance in removing the potential isobaric interference from  $^{26}\text{Mg}$  (11% natural abundance). Thus, although the molecular  $\text{AlO}^-$  beam is generally far more intense than the  $\text{Al}^-$  beam, the former species is not selected in our application because the analogous  $\text{MgO}^-$  are stable, and formed as readily as  $\text{AlO}^-$ , so that the discrimination against the  $^{26}\text{Mg}$  isobar would

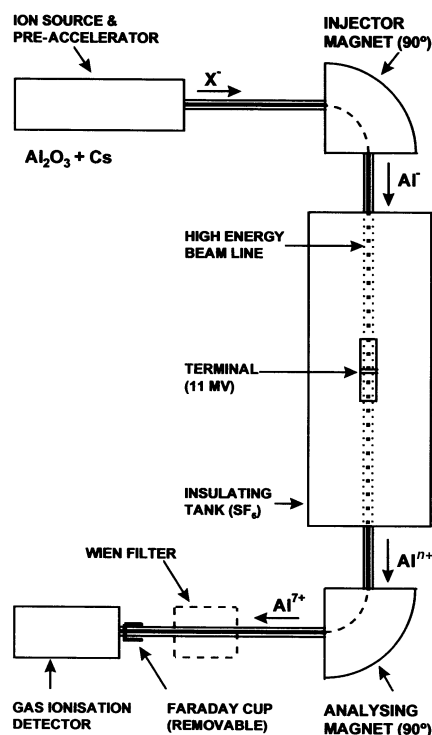


Fig. 1 The accelerator mass spectrometer system at the Australian National University (note the position of the recently introduced Wien filter in the detector beam line).

be lost (an alternative approach which has been used previously<sup>9</sup> is to select the molecular ion beam and fully strip the metals to  $\text{Al}^{13+}$  and  $\text{Mg}^{12+}$ , which can be separated in a magnetic spectrometer). More modern high intensity sources can produce  $\text{Al}^-$  beams up to  $1 \mu\text{A}$ ,<sup>19</sup> and a source of this type, with a 32-position sample wheel, is now in use at ANU.

### Sample material

Although metallic aluminium would in principle be the ideal ion source material for aluminium AMS, for biological work the oxide or phosphate is more convenient as these compounds are readily prepared from organic matrices, whereas production of the metal would be more problematic. However, both these compounds are thermal and electrical insulators, and function much more effectively when mixed with silver powder, which prevents the build-up of surface charge and removes heat by conduction. We have shown earlier that beam currents obtained from alumina samples mixed with silver powder passed through a well defined maximum between 50 and 80% Ag.<sup>9</sup> Aluminium oxide or phosphate samples are, therefore, mixed with an approximately equal mass of silver powder before pressing, although for very small samples ( $< 1 \text{ mg}$ ) much higher ratios of silver powder ranging from 1 : 2 up to 1 : 10 are used to bulk out the sample.

In order to reduce the possibility of cross-contamination between samples, and to obtain measurements with reasonable counting statistics, the amount of  $^{27}\text{Al}$  added to each sample is adjusted on the basis of an estimate of  $^{26}\text{Al}$  content, to generate an isotope ratio ( $^{26}\text{Al}/^{27}\text{Al}$ ) in the range  $10^{-8}$ – $10^{-12}$ . To produce stable and sustainable  $\text{Al}^-$  beam currents, the amount of  $^{27}\text{Al}$  is optimally at least 1 mg, although measurements have been obtained with amounts down to 0.1 mg bulked out with powdered silver.

### Measurement of Isotopes

#### Detection of $^{26}\text{Al}$

The gas ionisation chamber used for this work has been described previously<sup>17</sup> (see Fig. 2). Propane (about 150 Torr) is retained in the detector by a  $1.5 \mu\text{m}$  thick Mylar window. Incoming high energy ions pass through the window (energy loss  $\approx 3\%$ ) and traverse the length of the detector between a planar cathode and a parallel, segmented anode. The passage of the ions through the gas produces ionisation of some of the gas molecules and the electrons produced move under the influence of the applied electric field. Signals are taken from the cathode and from the various segments of the anode plane. The cathode signal is proportional to the intensity of gas ionisation, hence the total deposited energy, while each of the anode signals is

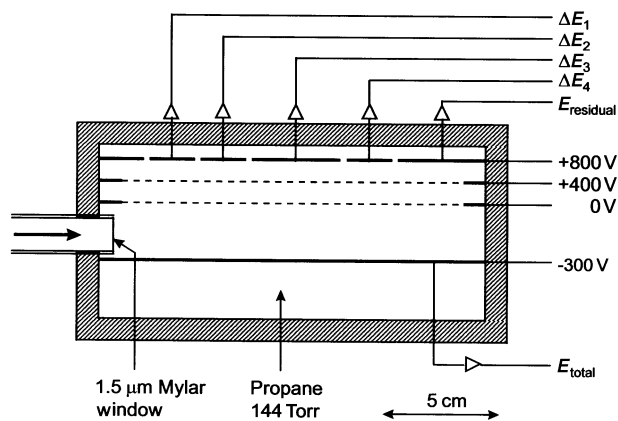


Fig. 2 The gas ionisation detector.

proportional to the energy deposited in the region of space adjacent to the segment in question. At the energies available from tandem accelerators, the rate of energy loss depends on both the nuclear charge and instantaneous kinetic energy of the ion, and hence a particular combination of total energy and differential energy loss is characteristic of a particular isotopic species. This is illustrated in Fig. 3, which shows a two-dimensional representation of some typical  $^{26}\text{Al}$  data. Note that, despite the high level of discrimination implicit in the AMS system,  $^{26}\text{Al}$  ions are far from being the only ions to reach the detector, and the ion identification capability of the detector is crucial. Whilst the initial data analysis is carried out against the two variables depicted in Fig. 3, further discrimination can be obtained by the application of the energy loss rate parameters, which essentially add additional dimensions to the spectral analysis.

#### Other ions reaching the detector

Other ionic species result from the fragmentation of mass 26 molecular ions (e.g.,  $^{10}\text{B}^{16}\text{O}^-$ ,  $^{12}\text{C}^{14}\text{N}^-$ ,  $^{25}\text{Mg}^+\text{H}^-$  and  $^{24}\text{Mg}^{2+}\text{H}^-$ ), and may arrive at the detector as a result of a fortuitous combination of circumstances which has a very low but finite probability. Specifically, following dissociation and stripping in the high-voltage terminal, a very small fraction undergoes a charge-changing collision with a residual gas molecule during the second stage of acceleration. If this occurs at just the right place, the ion can acquire the correct energy to pass round the final magnetic analysis and hence to the detector. For example, for an  $^{16}\text{O}$  ion to reach the detector, it must be injected as the  $\text{BO}^-$  molecular ion, dissociated and stripped to  $3+$  in the terminal and then charge exchanged to  $4+$  after it has experienced 37% of the second stage of acceleration. Although under normal circumstances these ions are easily distinguished from  $^{26}\text{Al}$ , if their arrival rate is sufficiently rapid there is a significant probability that a second ion will enter the detector within the time taken ( $2 \mu\text{s}$ ) to collect the electrons deposited by the passage of the first. Under these conditions, the pulses from the detector electrodes will overlap ('pile up'), and the total energy and energy loss measurements will exhibit a spread of values ranging from the values for a single ion up to the values for the sum of the two ions, depending on their relative times of arrival. This pile-up produces a non-zero background over a wide area of the 2-D spectrum (e.g., Fig. 3), including the  $^{26}\text{Al}$  region, and for this reason it is desirable to keep the rates low. Thus, in the past particular attention has been paid in the production of the source material to eliminate sources of B, C and N, and to reduce Mg concentrations to as low as is practicable. However, most of the problems relating to extraneous ions can also be eliminated by including a velocity

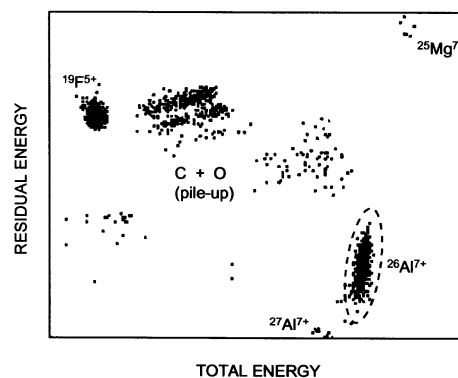


Fig. 3 Two-dimensional representation of a typical  $^{26}\text{Al}$  mass spectrum obtained in the absence of the Wien filter. With the filter in operation, only  $^{26}\text{Al}$  (shown in the defining ellipse) is observed in the 2-D spectrum.

filter before the detector, and the effect of this modification is described below.

#### Wien filter

A recent addition to the system is a final analysis stage consisting of crossed electric and magnetic fields, which functions as a velocity filter (commonly termed a Wien filter) and is included between the analysing magnet and the detector. This is set to allow  $^{26}\text{Al}$  ions to pass undeflected, but other ions which have different velocities are deflected out of the beam line and thus do not reach the detector.

All of the data presented in this paper were obtained prior to the installation of the Wien filter. Subsequent experience with this device has shown that it is extremely effective in preventing any ions except  $^{26}\text{Al}$  from reaching the detector, *i.e.*, the spectrum equivalent to Fig. 3 now contains only the  $^{26}\text{Al}$  group and nothing else. It follows that in the future it will be less necessary to reduce levels of B, C, N and Mg in the sample preparation.

#### Detection of $^{27}\text{Al}$

Measurements of the two isotopes,  $^{26}\text{Al}$  and  $^{27}\text{Al}$ , are made sequentially. The  $^{27}\text{Al}$  component of the sample is determined by measuring the  $^{27}\text{Al}^{7+}$  beam current impinging on a Faraday cup placed immediately in front of the detector window, during the phase of the operating cycle when the field of the injector magnet and terminal potential have been adjusted to transmit  $^{27}\text{Al}^{7+}$  through the machine. This adjustment is relatively slow (about 15 s), so that the precision with which the isotope ratio can be determined is highly dependent on the stability of the Al beam. In practice, the  $^{27}\text{Al}^{7+}$  beam is integrated for a period of up to 20 s before, during and after every  $^{26}\text{Al}$  counting period (usually 300–600 s). Because there is no method of monitoring beam current during the  $^{26}\text{Al}$  counting phase, the effective  $^{27}\text{Al}$  beam current during each counting period is taken as the mean of the two spanning measurements. The error associated with measurement of  $^{27}\text{Al}$  intensity is probably one of the more important factors limiting the precision of isotope ratio measurement.

#### Determination of the $^{26}\text{Al}/^{27}\text{Al}$ atom ratio

Most laboratories measure the  $^{26}\text{Al}/^{27}\text{Al}$  ratios of samples relative to a standard of known ratio. This has the obvious advantage that variations in machine performance that might affect the transmission of the  $^{26}\text{Al}$  and  $^{27}\text{Al}$  beams differentially are nullified. However, the method has the disadvantage that the accuracy of the ratio determinations for the samples in any particular run is limited by the accuracy of the calibration measurement for that particular run. However, because in our system the two beams traverse identical paths through the machine, it is possible to adopt an alternative approach, and to make a quasi-absolute measurement of isotope ratio. Thus, both the  $^{26}\text{Al}$  and  $^{27}\text{Al}$  intensities can be measured by reference to a primary physical quantity, namely time or current, respectively: the  $^{26}\text{Al}$  atoms are individually counted by the detector and the  $^{27}\text{Al}$  beam current is measured directly. Provided that the different stripping efficiencies of the two isotopes (0.339 for  $^{27}\text{Al}^{7+}$  at 11.00 MeV and 0.312 for  $^{26}\text{Al}^{7+}$  at 11.42 MeV) are taken into account, the isotope ratio can then be calculated. We adopted this approach, and merely use concurrent measurements on a reference material ( $^{26}\text{Al}$  doped  $\text{Al}_2\text{O}_3$ , of known  $^{26}\text{Al}/^{27}\text{Al}$  ratio) to monitor both the short and long term stability of the system. The accuracy and precision of measurement are considered below (see Instrumental Performance).

## Instrumental Performance

### Baseline

It should be emphasised that, in contrast to most other analytical techniques, including conventional mass spectrometry, AMS can be background free. In the absence of detector pile-up, if no  $^{26}\text{Al}$  ions reach the detector, no counts will be recorded in the  $^{26}\text{Al}$  region of the 2-D spectrum. The detection limit is determined, therefore, not by an unresolvable background, but by the output and efficiency of the ion source, the efficiency of transmission through the AMS system and the period of the observation (which affects the statistics of counting). For measurements carried out on pure aluminium oxide (*i.e.*, no  $^{26}\text{Al}$ ; a 'machine blank'), over a 600 s counting period, it is rare that more than one count will be recorded, corresponding to a nominal  $^{26}\text{Al}/^{27}\text{Al}$  ratio of about  $10^{-14}$ . Under these circumstances, the lower limit to the useful range of measurement is about  $10^{-13}$ , as in practice it is only above this ratio that the precision of measurement ceases to be determined by the statistics of counting. However, this limit is more than adequate for most biomedical applications.

### Accuracy and precision of measurement

As described previously, sample  $^{26}\text{Al}/^{27}\text{Al}$  ratios are determined absolutely, without the need for instrument calibration. However, to test the accuracy of this procedure, and to determine short and long term reproducibility of measurement, the isotope ratio of a standard material ( $^{26}\text{Al}$ -containing  $\text{Al}_2\text{O}_3$ ) is generally measured within each 12-sample set. The standard (supplied by S. Vogt, Purdue University, USA) was prepared by serial dilution of an  $^{26}\text{Al}$  stock solution, originally characterised by gamma spectrometry, and the calculated  $^{26}\text{Al}/^{27}\text{Al}$  ratio is  $2.78 \times 10^{-10}$  (subject to an estimated uncertainty of 4%, mainly arising from the uncertainty with which the radioactive half life of  $^{26}\text{Al}$  has been determined). The mean value determined by AMS over 4 years (Table 2) is  $2.75 \times 10^{-10}$  (RSD 6.5%,  $n = 66$ ), in good agreement with the nominal value. However, the absolute accuracy of measurement is never an issue in biomedical applications involving the use of isotopic tracers, as the  $^{26}\text{Al}$  content of the original tracer is always determined alongside the working samples, and experimental results are thus internally calibrated.

The precision of the measurement technique was determined from repeat measurements on the calibration material during the course of a single run, *i.e.*, a measurement period where the overall tuning of the accelerator is not altered. Under these circumstances, the RSD of a number of measurements of  $^{26}\text{Al}/^{27}\text{Al}$  ratio varies between 3 and 6% ( $n = 6$ ).

### Cross-contamination

Cross-contamination between samples can occur in the ion source. This possibility was investigated by placing aluminium

**Table 2** Repeat measurements on the  $^{26}\text{Al}/^{27}\text{Al}$  standard over a 4 year period. The values obtained show a normal distribution, with a mean value of  $2.75 \times 10^{-10}$  (RSD = 6.5%,  $n = 66$ ), not significantly different from the nominal value ( $2.78 \times 10^{-10}$ ; S. Vogt, unpublished). There has also been no significant drift over this period, as is demonstrated by the means for each sequential 12 month period

Year	Number	Mean	RSD (%)
1992–93	16	2.69	4.99
1993–94	19	2.69	5.50
1994–95	11	2.67	7.65
1995–96	20	2.91	4.06
All years	66	2.75	6.47

oxide samples of widely differing  $^{26}\text{Al}/^{27}\text{Al}$  ratios ( $< 10^{-14}$  and  $10^{-10}$ ) in neighbouring positions in the sample wheel. The blank sample was measured for a 20 min period both before and after sputtering the higher level sample for the same period. The blank was not significantly affected by the sputtering of the higher ratio sample, recording 0 and 1 count for the two measurements, respectively, where 1 count would correspond to a ratio  $^{26}\text{Al}/^{27}\text{Al} = 3 \times 10^{-14}$ . This implies that cross-contamination was in this instance  $\leq 1$  part in  $10^4$ .

### Interferences

$^{26}\text{Mg}$  (11% of natural Mg) is the only stable nuclide isobaric with  $^{26}\text{Al}$ , and presents a potential problem of interference, as magnesium is usually a major constituent of biological materials and the  $^{26}\text{Mg}/^{26}\text{Al}$  ratio in typical unprocessed samples may range from  $10^8$  to  $10^{12}$ . Selective isolation of Al during sample preparation may reduce this ratio by 3–4 orders of magnitude (see later), but the Mg content of the final sample material is invariably far higher than the  $^{26}\text{Al}$  content. Two factors help to eliminate the isobaric interference. First, the  $\text{Mg}^-$  ion is unstable, and  $^{26}\text{Mg}^-$  ions do not survive long enough to reach the high voltage terminal of the accelerator. Hence  $^{26}\text{Mg}^-$  is effectively eliminated by the ion source. In principle, a low energy tail on the  $^{26}\text{MgH}^-$  beam could permit a very small fraction of  $^{26}\text{Mg}^-$  containing molecular ions to pass the injector magnet and undergo the first stage of acceleration. However, the  $^{26}\text{Mg}$  component of this molecular ion arrives at the terminal with only 96.3% (*i.e.*, 26/27) of the energy of the  $^{26}\text{Al}^-$  ions. Hence, following stripping, the  $^{26}\text{Mg}$  ions must undergo charge-changing collisions during the second stage of acceleration in order to reach the detector. In practice,  $^{26}\text{Mg}$  ions have not been observed in the detector, and this sequence of events must have an extremely low probability.

Molecular ions of the lighter Mg isotopes,  $^{25}\text{MgH}^-$ ,  $^{24}\text{MgH}_2^-$  and  $^{24}\text{Mg}^2\text{H}^-$ , are all accepted by the injector magnet at  $m/z$  26. Again,  $^{24}\text{Mg}$  and  $^{25}\text{Mg}$  ions can only reach the detector as a result of charge-changing collisions, but these ions have been observed. In practice,  $^{25}\text{Mg}$  ions are substantially more abundant at the detector than  $^{24}\text{Mg}$  ions, although counting rates rarely exceed  $10 \text{ s}^{-1}$ , and the detector provides excellent discrimination from  $^{26}\text{Al}$  (Fig. 3).

In order to confirm experimentally that Mg in the sample does not produce interference with the  $^{26}\text{Al}$  signal, six  $\text{Al}_2\text{O}_3$  samples were prepared, three containing  $^{26}\text{Al}$  and four containing Mg (see Table 3). The measured  $^{26}\text{Al}/\text{Al}$  ratios are apparently unaffected by the presence or otherwise of Mg, up to an Mg/Al ratio of 1:40.

The other potential interference (*i.e.*, effect producing spurious counts which might be assigned to  $^{26}\text{Al}$ ) is ion pile-up in the detector; the basis for the phenomenon was described earlier. Pile-up is generally caused by the arrival of high intensities of C, N and O positive ions at the detector, resulting in turn from the transmission of mass 26 molecular ions (*e.g.*,  $\text{BO}^-$ ,  $\text{CN}^-$ ) to the terminal. Residual C and N in samples results

from incomplete oxidation of organic matter, and high B levels may result from leaching of borosilicate glass vessels during acid digestion stages. The effects of pile-up can be reduced by careful attention to the chemistry of the final stages of sample preparation, including the use of acid-etched glassware (to remove leachable boron) and prolonged high temperature ignition, if necessary in an oxygen-enriched atmosphere, of the final aluminium oxide preparation (to remove traces of carbon). However, the recent introduction of a Wien filter in the system has greatly reduced the stringency of the chemical requirements in this respect.

## Analysis of Biological Materials

### Sample Preparation

#### General principles

Sample preparation in this context consists of the conversion of a biological material into an amount of aluminium oxide or phosphate suitable for presentation as an ion source. It is assumed that the biological part of the experiment has been appropriately designed, to yield samples containing at least  $10^{-16} \text{ g}$  of  $^{26}\text{Al}$  and not more than about  $10 \mu\text{g}$  of  $^{27}\text{Al}$ . The preparation procedure consists essentially of four stages: (i) addition and homogenisation of  $^{27}\text{Al}$  carrier; (ii) removal of, or separation from, the organic matrix; (iii) isolation of aluminium from the inorganic matrix; and (iv) conversion of the aluminium-containing fraction to dry aluminium oxide or phosphate.

Aluminium of natural isotopic abundance (*i.e.*,  $^{27}\text{Al}$ ) is normally added, as an aliquot of an acidic solution, to a known mass/volume of the raw sample material, prior to any chemical treatment. The Al acts as an isotope carrier, and the amount added is determined on three criteria: first, the amount must be significantly greater (ideally, at least 100 times) than the natural Al already present in the samples; second, the desirable range for the final  $^{26}\text{Al}/^{27}\text{Al}$  ratio in measured material is from  $10^{-12}$  to  $10^{-8}$ ; and third, the minimum amount of  $\text{Al}_2\text{O}_3$  which can be employed, and which will produce a stable  $\text{Al}^-$  beam for at least 30 min, is about  $100 \mu\text{g}$ . Because the amount of  $^{26}\text{Al}$  tracer used in the biological experiments is likely to have been decided in the design of the experiment, the appropriate amount of  $^{27}\text{Al}$  carrier will normally fall in the range 1–10 mg (if, unusually, it is required to determine the  $^{26}\text{Al}/\text{Al}$  isotope ratio in the original biological sample, the  $^{27}\text{Al}$  concentration in the biological sample must, of course, be determined before the addition of carrier). Homogenisation of added  $^{27}\text{Al}$  with the sample  $^{26}\text{Al}$  is achieved by conversion of the entire sample into inorganic form in solution, concurrently with the removal of the organic matrix by nitric acid oxidation at elevated temperature. It is clearly important to ensure that no fractionation of Al isotopes can occur prior to this stage, when their chemical forms may be different.

Removal of the organic matrix and isolation of Al from other inorganic components is required both to reduce the dilution factor (*e.g.*, if a large amount of sodium or calcium is present) and, specifically, to reduce the Mg content to a tolerable level (target level  $< 1\%$ ). The organic components are normally oxidised by digestion with concentrated nitric acid at elevated temperature and pressure, using microwave heating. Methods employed to extract Al from the strongly acidic residue, depending on circumstance, are selective precipitation of Al as the 8-hydroxyquinoline derivative<sup>20</sup> or solvent extraction of Al as the acetylacetonate.<sup>21</sup> In each case, once the Al component has been isolated as a solid phase, high temperature ashing in a muffle furnace (with oxygen flow if necessary) is generally sufficient to produce the ion source material.

The purities of the Al compounds produced were estimated by elemental analysis (ICP-OES for Al, Mg, Ca, Na and K), and the stepwise and overall yields were determined using  $^{26}\text{Al}$

**Table 3** Test of the effect of added Mg on the AMS determination of the  $^{26}\text{Al}$  content of  $\text{Al}_2\text{O}_3$  containing an aliquot (Y) of  $^{26}\text{Al}$

$^{26}\text{Al}$	$10^6(^{26}\text{Mg}/\text{Al})$	$10^{12}(^{26}\text{Al}/^{27}\text{Al})$ (measured)
0	0	$< 0.1$
0	2.5	$< 0.1$
0	2.5	$< 0.1$
Y	0	238
Y	2.5	249
Y	2.5	238

tracer and radiochemical methods (liquid scintillation counting and gamma spectrometry). In most circumstances, the overall yields are 70–90% and metal atom impurities below 1% (*i.e.*, given as atom ratios relative to Al), which are generally satisfactory. Provided that sufficient material is produced to make an ion source, the chemical processing yield has no effect on the accuracy of the AMS determination, as once the  $^{27}\text{Al}$  carrier has been added the  $^{26}\text{Al}/^{27}\text{Al}$  isotope ratio will not alter significantly in the subsequent chemical processing. In all preparations described below, analytical-reagent grade reagents (AnalaR grade, BDH/Merck, Poole, Dorset, UK) were employed, and acid leached, previously unused glass- or plastic-ware was employed for  $^{26}\text{Al}$  sample preparations.

#### Blood and soft tissues

Blood and plasma sample volumes were typically in the range 1–5 ml and the soft tissue mass was normally less than 10 mg. The relatively small size of the biological samples allowed the removal of organic matter by oxidation under pressure with concentrated nitric acid [10 ml at 180 °C at about 10 bar, using a CEM (Matthews, NC, USA) Model 2000 microwave digestion system], following the addition of the appropriate amount of  $^{27}\text{Al}$  carrier (usually 1–5 mg Al). The resulting strongly acidic solutions were evaporated to dryness in acid leached glass beakers on a hot-plate. The residue was dissolved in hot nitric acid (1 M; 10 ml), transferred into a 50 ml centrifuge tube and treated with sodium acetate (1 M, 10 ml, as a pH buffer) and a substantial excess of 8-hydroxyquinoline<sup>20</sup> (5% in 2 M acetic acid, using 5 ml per 1 mg of  $^{27}\text{Al}$ ). The pH was then adjusted to 5.8 with concentrated ammonia solution and the precipitated aluminium 8-hydroxyquinolate separated by centrifugation, washed with distilled water and dried at 120 °C. The material was transferred into a porcelain crucible and converted into aluminium oxide by heating in air in a muffle furnace (raised slowly to 800 °C and held for 8 h). The application of this technique allowed the separation of Al from Na, K, Mg and Ca present in the original blood/tissue. Aluminium starts to form a neutral complex with 8-hydroxyquinoline at about pH 4.5, and this is precipitated quantitatively above pH 5.5. Although Mg and Ca form complexes with 8-hydroxyquinoline, it is claimed<sup>20</sup> that these compounds do not precipitate appreciably at this pH, and we confirmed this in our chemical systems (see Fig. 4). Analysis of the 8-hydroxyquinoline precipitate showed the Al yield to be about 90% (based on the original  $^{27}\text{Al}$  addition), with contamination by Mg or Ca below 1% (atom ratio *versus* Al).

#### Urine

Urine samples (generally 24 h collections) were acidified with nitric acid (10 ml of acid per litre of urine) and refrigerated. The

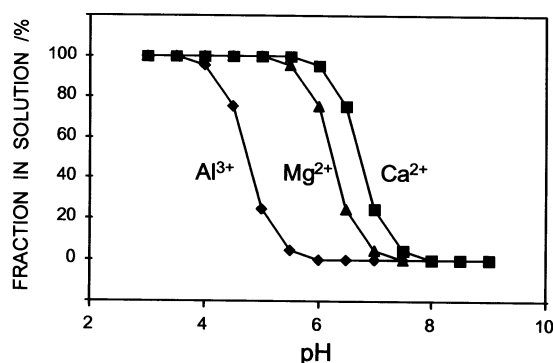


Fig. 4 pH dependence of 8-hydroxyquinoline precipitation for  $\text{Al}^{3+}$ ,  $\text{Ca}^{2+}$  and  $\text{Mg}^{2+}$

first stage of the extraction method was designed to remove aluminium from the organic material, by the coprecipitation of aluminium, calcium and magnesium phosphates, using the calcium and magnesium naturally present in the urine (normally about 2.5–7.5 and 3.3–4.9 mmol d<sup>-1</sup> respectively). The appropriate amount of  $^{27}\text{Al}$  carrier (5–50 mg) and a large excess of sodium phosphate (1 M  $\text{NaH}_2\text{PO}_4$  at 20 ml per litre of urine) were added and the solution was heated at 80 °C for 30 min to bring any solids present into solution. After cooling to room temperature, the solution was brought to pH 8–9 with 6 M ammonia solution. After about 12 h, the mixed phosphate precipitate was isolated by decantation and centrifugation of the solution and was then redissolved in nitric acid (8 M; 20 ml). Citric acid (6 g) was added and the pH brought to 5.5 by the addition of ammonia solution (the citric acid just prevents the precipitation of calcium phosphate at this pH). Pentane-2,4-dione (acetylacetone) (5 ml) was added and the mixture shaken vigorously for 5 min, followed by 2-methylbutan-1-one (isobutylmethyl ketone; IBMK) (15 ml). Following phase separation (assisted by mild centrifugation if necessary), the organic layer was removed, further IBMK (15 ml) added and the phases separated. The yield of Al at this point is about 70% (see Table 4), the loss of Al occurring probably because some is trapped by the calcium phosphate solid which precipitates. To recover this, the aqueous solution was re-acidified (nitric acid) to dissolve the precipitate, and the entire extraction procedure repeated, giving an overall yield of about 90–95%. Aluminium was recovered by back-extraction from the combined organic phase with nitric acid (1.0 M; two portions of 10 ml). The aqueous phase was washed with two portions of IBMK (5 ml) to remove any residual acetylacetone, and subsequently evaporated to dryness on a hot-plate in a small beaker. Two portions of nitric acid (16 M; 5 ml) were added sequentially to the residue, each followed by boiling and evaporation to dryness, and the final residue was heated to high temperature (about 300 °C) on the hot-plate. The dry residue (which was grey-white) was converted into  $\text{Al}_2\text{O}_3$  (white) by ignition at 800 °C as described previously (the overall yield from  $^{27}\text{Al}$  added to original urine was 70–90%).

#### Performance Characteristics

##### Detection limits

The lower limit of ratio measurement, as discussed earlier, is around  $10^{-14}$ . Measurements at this level could be made without undue difficulty on samples containing 0.1 mg of  $^{27}\text{Al}$ , implying a detection limit of about  $10^{-18}$  g of  $^{26}\text{Al}$  (about 20 000 atoms).

##### Linear range

The physics of measurement determine that the response is essentially linear. The upper limit of practicable measurement is determined by the saturation rate of the gas ionisation detector, about  $10^4$  counts  $\text{s}^{-1}$ . The lower limit, as discussed earlier, is

Table 4  $^{26}\text{Al}$  recovery by acetylacetone extraction from calcium phosphate solution (organic phase, IBMK; aqueous pH, 5.5, containing excess citric acid)

Operation	$^{26}\text{Al}$ recovered (%)
First extraction (2)	70
Second extraction (2)	25
Total organic phase	95
Back-extraction (2)	95
Residual, aqueous phase	< 3
Residual, organic phase	< 3

**Table 5** Reproducibility test: fivefold replicate determination of the  $^{26}\text{Al}/^{27}\text{Al}$  ratio in a sample of blood plasma

Sample No.	$10^{10}(^{26}\text{Al}/^{27}\text{Al})$	SD*
1	2.40	0.10
2	2.28	0.10
3	1.98	0.13
4	2.23	0.15
5	2.01	0.11
Mean:	2.18	
$s^\dagger$	0.18	
RSD (%)	8.26	

\* Standard deviation of the measurement based on counting statistics for  $^{26}\text{Al}$ .  $^\dagger$  Standard deviation of the measurements based on the observed variability.

about  $10^{-3}$  counts  $\text{s}^{-1}$ , determined by the detector background and the practicable limits to counting time. The measurement range thus covers seven orders of magnitude, corresponding to a  $^{26}\text{Al}/^{27}\text{Al}$  isotope ratio, from  $10^{-14}$  to  $10^{-7}$ .

### Precision

The short and long term reproducibility of measurement based on repeated determinations of the  $^{26}\text{Al}/^{27}\text{Al}$  ratio of a calibration material have already been reported (Table 2). The RSD over 4 years is approximately 6.5%, and this figure may be taken to represent the precision of measurement of the machine itself over a long period. In order to gauge the reproducibility of measurement on a real sample material, five independent repeated measurements on a blood plasma sample containing a moderate level of  $^{26}\text{Al}$  were made, using the method described earlier. The results (Table 5; RSD = 8.3%) show a slightly larger variability than those for the calibration material, and this figure probably represents the reliability of measurement on a real sample under relatively good conditions.

This work was supported (in part) by Withington Hospital Renal Unit Endowment Fund, the Royal Society (London) and the Engineering and Physical Sciences Research Council, UK. Accelerator facilities at the Australian National University were provided under the EPSRC/ANU Joint Agreement.

### References

- 1 Flaten, T. P., Alfrey, A. C., Birchall, J. D., Savory, J., and Yokel, R. A., *J. Toxicol. Environ. Health*, 1996, **48**, 527.

- 2 Litherland, A. E., *Philos. Trans. R. Soc. London, Ser A*, 1987, **323**, 5.
- 3 Day, J. P., Barker, J., King, S. J., Miller, R. V., Templar, J., Lilley, J. S., Drumm, P. V., Newton, G. W. A., Fifield, L. K., Stone, J. O. H., Allan, G. L., Edwardson, J. A., Moore, P. B., Ferrier, I. N., Priest, N. D., Newton, D., Talbot, R. J., Brock, J. H., Sanchez, L., Dobson, C. B., Itzhaki, R. F., Radunovic, A., and Bradbury, M. W. B., *Nucl. Instrum. Methods Phys. Res., Sect. B*, 1994, **92**, 463.
- 4 Fifield, L. K., Ophel, T. R., Bird, J. R., Calf, G. E., Allison, G. B., and Chivas, A. R., *Nucl. Instrum. Methods Phys. Res., Sect. B*, 1987, **29**, 114.
- 5 Reedy, R. C., Tuniz, C., and Fink, D., *Nucl. Instrum. Methods Phys. Res., Section B*, 1994, **92**, 335.
- 6 Hedges, R. E. M., *Nucl. Instrum. Methods Phys. Res., Sect. B*, 1990, **52**, 428.
- 7 Vogel, J. S., and Turteltaub, K. W., *Nucl. Instrum. Methods Phys. Res., Sect. B*, 1994, **92**, 445.
- 8 Elmore, D., Bhattacharyya, M. H., Sacco-Gibson, N., and Peterson, D. P., *Nucl. Instrum. Methods Phys. Res., Sect. B*, 1990, **52**, 531.
- 9 Barker, J., Day, J. P., Aitken, T. W., Charlesworth, T. R., Cunningham, R. C., Drumm, P. V., Lilley, J. S., Newton, G. W. A., and Smithson, M. J., *Nucl. Instrum. Methods Phys. Res., Sect. B*, 1990, **52**, 540.
- 10 Day, J. P., Barker, J., Evans, L. J. A., Perks, J., and Seabright, P. J., *Lancet*, 1991, **337**, 1345.
- 11 King, S. J., Day, J. P., Moore, P. B., Edwardson, J. A., Taylor, G. A., Fifield, L. K., and Cresswell, R. G., *Nucl. Instrum. Methods Phys. Res., Ser. B*, 1997, **123**, 254.
- 12 Priest, N. D., Newton, D., Day, J. P., Talbot, R. J., and Warner, A. J., *Hum. Exp. Toxicol.*, 1995, **14**, 287.
- 13 Priest, N. D., Talbot, R. J., Austin, J. G., Day, J. P., King, S. J., Fifield, L. K., and Cresswell, R. G., *Biometals*, 1996, **9**, 221.
- 14 Fifield, L. K., Cresswell, R. G., di Tada, M. L., Ophel, T. R., Day, J. P., Clacher, A. P., King, S. J., and Priest, N. D., *Nucl. Instrum. Methods Phys. Res., Sect. B*, 1996, **117**, 295.
- 15 Fifield, L. K., Clacher, A. P., Morris, K., King, S. J., Cresswell, R. G., Day, J. P., and Livens, F. R., *Nucl. Instrum. Methods Phys. Res., Ser. B*, 1997, **123**, 400.
- 16 Fifield, L. K., Allan, G. L., Stone, J. O. H., and Ophel, T. R., *Nucl. Instrum. Methods Phys. Res., Sect. B*, 1994, **92**, 85.
- 17 Fifield, L. K., Ophel, T. R., Allan, G. L., Bird, J. R., and Davie, R. F., *Nucl. Instrum. Methods Phys. Res., Sect. B*, 1990, **52**, 233.
- 18 Brand, K., *Nucl. Instrum. Methods Phys. Res.*, 1977, **141**, 519.
- 19 Middleton, R., *Nucl. Instrum. Methods Phys. Res.*, 1984, **220**, 105.
- 20 Vogel, A., *A Textbook of Quantitative Inorganic Analysis*, Longmans, London, 1978, 3rd edn., p. 516.
- 21 Eshelman, H. C., Dean, J. A., Menis, O., and Rains, T. C., *Anal. Chem.*, 1959, **31**, 183.

Paper 7/02002C  
Received March 24, 1997  
Accepted June 16, 1997